VOL. 19, NO. 13, JULY 2024 ISSN 1819-6608
ARPN Journal of Engineering and Applied Sciences


www.arpnjournals.com

# CHARACTERIZATION OF DEVELOPED INTEGRATING SPHERE PHOTOMETER SYSTEM FOR TOTAL LUMINOUS FLUX MEASUREMENTS

Manal A. Haridy
Photometry and Radiometry Division, National Institute of Standards (NIS), Giza, Egypt
E-Mail: manal_haridi@yahoo.com

## ABSTRACT
This research focuses on characterizing a developed integrating sphere photometer system for measuring total luminous flux at the National Institute of Standards (NIS) in Egypt. The research examines factors such as the efficiency of the integrating sphere across different wavelengths, the sphere photometer calibration factor (SPCF), and temperature variations in the photometer system during measurement days. One setup utilizes a spectroradiometer with an uncertainty of 4.7% and a 2.5-meter integrating sphere to measure the spectral responsivity of the sphere photometer. Another setup involves a 2.5-meter big-integrating sphere and NIS-photometer, along with NIS- luminous flux standard lamps calibrated at (NPL) with an uncertainty of 0.8%, to determine the SPCF. The overall uncertainty of the final (SPCF) ranges from 0.03% to 0.05%, while the temperature variation during measurements ranges from 0.045% to 0.07%.

**Keywords:** uncertainty, the spectral efficiency of the integrating sphere, sphere photometer calibration factor (SPCF), spectral Responsivity of Sphere.

Manuscript Received 27 May 2024; Revised 27 July 2024; Published 20 September 2024

## 1. INTRODUCTION
The field of photometry holds a distinctive role within the realm of physics, serving as a subset of optical radiometry with influences from vision science. Its purpose is to accurately measure and characterize the properties of light [1]. The measurement of a light source's total luminous flux is commonly conducted using either a goniophotometer or an integrating sphere [2-4]. Traditionally, goniophotometers are employed to establish the unit for total luminous flux [5]. Nevertheless, constructing and maintaining highly accurate goniophotometers can be challenging, involving a spacious dark room and expensive, precision positioning equipment. The process of collecting data at numerous points with a goniophotometer is time-consuming, and Usually, the Head of the photometer covers only a tiny portion of the whole spherical area: below 3% in point-to-point measurement and below 20% in continuous integration measurement. [6]. Due to the need to minimize the burning time of lamps, compromises are made on scanning intervals, impacting measurement accuracy and time. In contrast, integrating spheres offer immediate and continuous spatial integration, achieving nearly 100% coverage of the entire spherical area, presenting a significant advantage over goniophotometers. While goniophotometers require fewer characterization measurements, they pose mechanical challenges and demand considerable time for measurements. To overcome these challenges, the integrating sphere photometer system employs the standard substitution method. This approach accelerates measurements, reducing the time lamps need to be operational. Integrating sphere photometers enable swift measurements and are commonly employed. Measuring the luminous flux of light sources presents various challenges. These would include, but not be limited to, discrepancies between the relative spectral sensitivity of the sphere photometer and the V(λ) spectral luminous efficiency of the human eye [7].

ISSN 1819-6608
ARPN Journal of Engineering and Applied Sciences



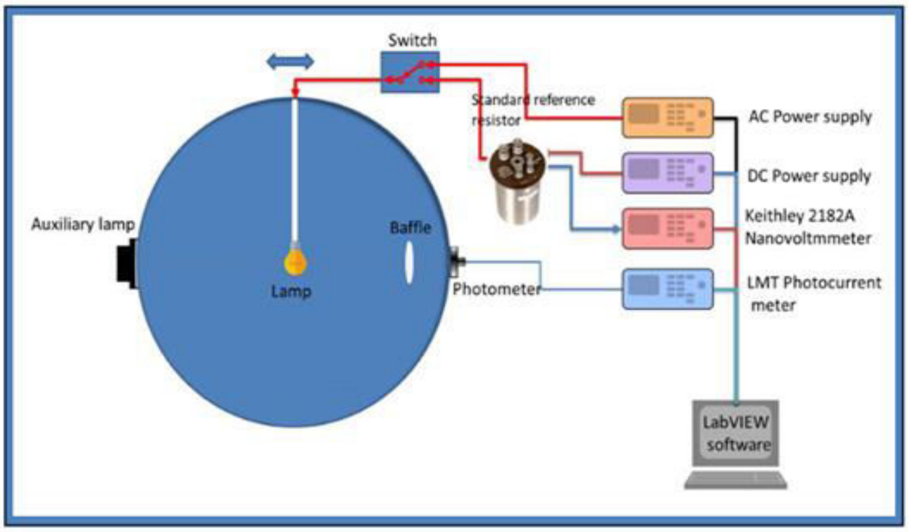


**Figure-1.** The luminous flux measurements set up at NIS [8].

The developed system consists of a 2.5-meter integrating sphere, an LMT U1000 photometer, a very stable and accurate power source, and standard reference luminous flux sources. The LabVIEW PID algorithm has been implemented in designing and controlling all instruments in the system [8]. The inner surface of the sphere is painted with Barium Sulphate paint, having a diffuse reflectance of about 97% in the visible range. Another 100 W tungsten lamp is mounted on the wall of the integrating sphere in order to measure self-absorption effects of lamps inside the sphere. The air temperature inside the sphere was monitored using a temperature sensor and was kept at about 25°C during lamp operation. [8]. The 2.5 meter integrating sphere at (NIS), equipped with the highly accurate Ocean Optics 2000 array Spectroradiometer, not only swiftly and precisely measures spectral power distributions within the 200nm-1100nm range but also computes and displays radiometric, photometric, and colorimetric parameters in accordance with CIE standard publications spanning 380nm-780nm. The NIS-Spectroradiometer comprises the unit, including the optical fiber [8]. In this study, I employed a configuration utilizing the NIS Spectroradiometer and an integrating sphere, was employed to gauge the spectral responsivity of the NIS integrating sphere. Additionally, another arrangement, utilizing the 2.5 m integrating sphere system and a photometer equipped with luminous flux standard lamps was utilized to determine the SPCF and estimate the associated uncertainties.


**Figure-2.** LABVIEW software control system for total flux developed NIS-integrating sphere photometer system [8].

ARPN Journal of Engineering and Applied Sciences




## 2. EXPERIMENTS AND MEASUREMENTS

The spectral responsivity of the sphere-photometer was established by multiplying the relative spectral throughput of the integrating sphere by the photometer head's relative sensitivity. To determine the spectral responsivity of the integrating sphere, the spectral distribution measured at the photometer port of one total flux working standard lamp was compared to that measured directly from the working standard lamp using the photometric bench and the spectroradiometer ocean optics HR 2000 at NIS, with an uncertainty of 4.7%. The experimental setup for measuring the sphere-photometer spectral responsivity is illustrated in Figure-3. The electrical parameters of NIS secondary standards lamps are represented in [9].

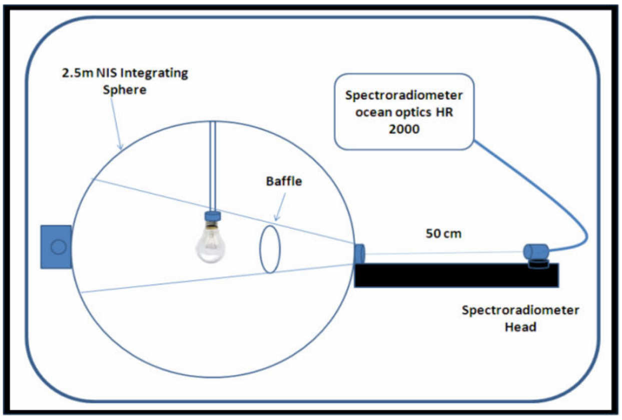


**Figure-3.** Illustrating the setup of the spectral responsivity measurement system.

The integrating sphere used has a diameter of 2.5 meter and is coated internally with a uniform layer of barium sulfate ( $BaSO_4$ ). The baffle is coated with a uniform layer of barium sulfate ( $BaSO_4$ ), and suspended on wire supports from the wall of the sphere and was situated approximately halfway between the lamp and the photometer port. The direct exposure of the photometer head is blocked using a small baffle between the lamp and the detector head. When using standard lamps, the test lamp is calibrated against a standard lamp of the same color temperature and the same size. Otherwise, spectral and spatial corrections are needed. It has been chosen to consider that the standard lamps calibrate the sphere photometer to give Sphere-Photometer Calibration Factor (SPCF) that may vary over time [9-11].

## 3. RESULTS AND DISCUSSIONS

Figure 4 illustrates in detail the relative spectral responsivity of the integrating sphere photometer developed at NIS. It was determined by separate measurements of two crucial parts: the relative spectral throughput of an integrating sphere. Such measurements have been very important because they enable more accurate understanding of how each part of the system contributes to the whole performance of the photometer. The relative spectral responsivity of the integrating sphere can be derived by calculating the ratio between the responsivity of the photometer and the throughput of the sphere. This will, in turn, give a complete measure of system performance over a range of wavelengths. In addition, spectral throughput of the integrating sphere was measured directly to further enhance the accuracy of the overall assessment of the system. Such measurements will help ensure that the integrating sphere photometer captures and quantifies luminous flux precisely across a range of wavelengths.

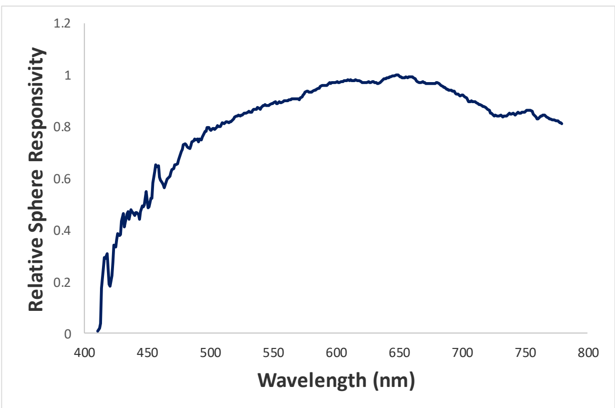


**Figure-4.** The spectral responsivity of the developed NIS-Integrating sphere.

Figures 5, 6, and 7 depict the performance of the developed SPCF showing the results of one-, two-, and three-consecutive-day measurements, respectively. The measurements are carried out day by day using standard lamps in order to test the responsivity of the integrating sphere every day. Figure 5 shows the measurement results of the first day's measurement, where the responsivity variation of the sphere has remained within 0.05; this means that the system response is pretty consistent, merely responding slightly to the standard lamps. Figure 6 shows the measurements done on the second day. It was similar in trend as the first one, but with a slight reduction in fluctuation of the responsivity of the sphere within 0.037. It may indicate that the system became more stable as time went on under the same conditions. Figure 7 presents data obtained by measurements on the third day, when the deviation in responsivity reduced to 0.03. The decrease in variation over three successive days points toward a developing consistency and reliability of the system. These curvature reports clearly present the sphere's performance; it shows that, with every day passing, the responsivity of the system becomes more stable. Gradual reduction in variability confirms the accuracy and repeatability of the integrating sphere photometer system-important features that guarantee precision in luminous flux measurement.

VOL. 19, NO. 13, JULY 2024 ISSN 1819-6608
ARPN Journal of Engineering and Applied Sciences



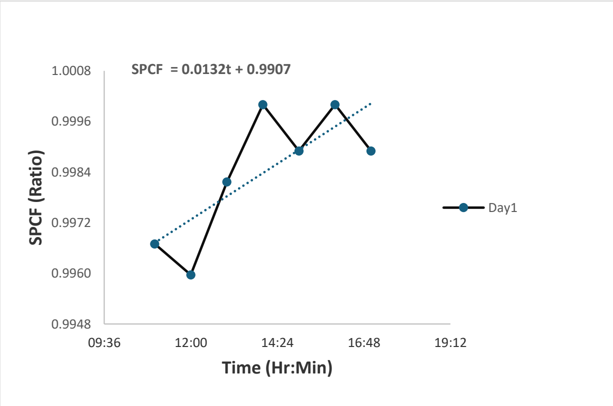


**Figure-5.** SPCF of standard lamps measured on the day one.

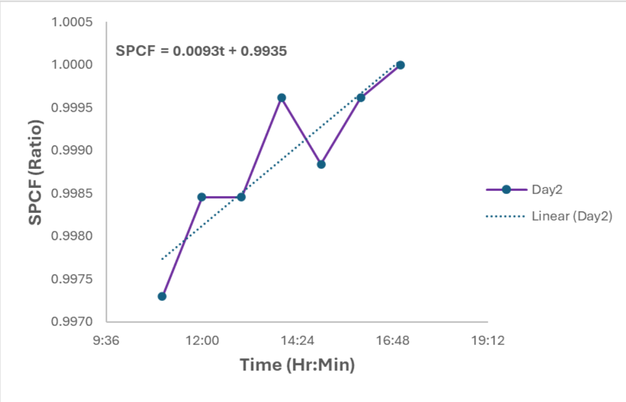


**Figure-6.** SPCF of standard lamps measured on the day two.

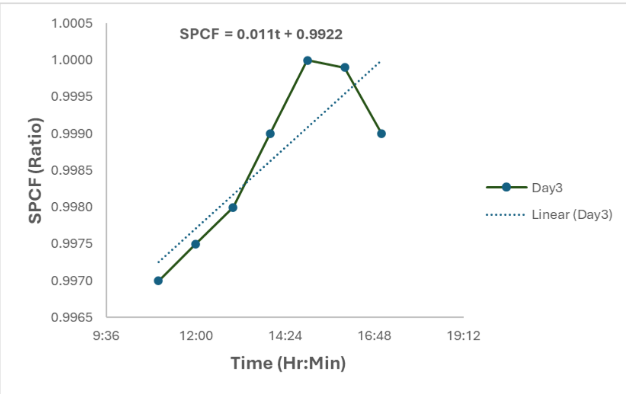


**Figure-7.** SPCF of standard lamps measured on the day three.

It was observed that the responsivity of the sphere photometer drifted during the day and that this drift could be mathematically characterized by a fit to the responsivity data with a linear trend. Figures 5, 6, and 7 show the fitted lines that describe the Sphere-Photometer Calibration Factor, SPCF, for the integrating sphere photometer system. Each of these equations has two core variables: SPCF and t. Here, SPCF = Sphere-Photometer Calibration Factor and t = the time of calibration that refers to a particular reading; The SPCF is given as a function of two parameters: Slope: This is the rate of variation of the SPCF of the lamp with every unit time elapsed. It describes how the responsivity of the sphere photometer system changes with time during the day. SPSCF intercept: This represents the value of SPCF at t = 0, actually a kind of initial calibration factor in the very beginning phase of measurement. These linear equations are important because they show the variation of the SPCF with time and hence describe the drift nature of responsivity. Of particular use are the curves obtained from fitted lines in Figures 5, 6, and 7. These were very useful to identify minor excursions of calibration that may take place over the day and correct it. They are a more stable way of calibration, allowing minute adjustments to improve the accuracy of measurement. First Day: The equation of the fitted line explains the gradual variation in SPCF during the measurement period to result in the observed drift. Similarly, the fitted line equations in Figures 6 and 7 for the second and third day also indicate a continued decrease in drift and thus enable increasingly finer calibrations. The equations for the three days can frame a method to achieve better calibration accuracy by adding time-dependent corrections to the Sphere-Photometer Calibration Factor in order to maintain consistent and reliable performance of the integrating sphere photometer system over long measurement periods.

$$SPCF = 0.0132t + 0.9907 \tag{1}$$

$$SPCF = 0.0093t + 0.9935 \tag{2}$$

$$SPCF = 0.011t + 0.9922 \tag{3}$$

Each figure provides an equation with two key variables, SPCF and t, where SPCF is the Sphere-Photometer Calibration Factor and t is a calibration time when the measurement is taken. The SPCF is expressed as a linear function that depends on two components: Slope-it shows the rate at which the SPCF changes with time and therefore gives an indication of how rapidly the calibration factor develops during the measurement period. SPCF intercept-this is the value of the calibration factor at t = 0 or, in other words, the baseline SPCF at the commencement of the measurement.

The relative spectral responsivity of photometers can be quite sensitive to the temperature of their optical components. If a photometer is not designed with temperature control, its use in ambient temperatures other than those during its calibration will introduce large measurement errors. Its performance is therefore affected since fluctuations in temperature might change the responsivity of the optical components and make the Sphere-Photometer Calibration Factor drift with time. For instance, if there is an on-lamp in the integrating sphere, the temperature increases with the heat being generated by the lamp. That same heat may affect the photometer head. As such, the response of a photometer would likely shift or drift due to this thermal effect. This drift in responsivity has a linear relationship with the temperature of the optics inside the photometer; if it is not taken into consideration, it may lead to errors in the measurement of luminous flux or other optical properties. To mitigate this effect, the linear equation models the SPCF drift with time and therefore permits real-time or post-measurement corrections. The ability to track the rate of variation of the SPCF gives an adjustment for an initial responsivity at the time of commencing the measurement, which allows the system to correct for temperature-induced errors so that data is more accurate and reliable-even while operating under variable thermal conditions. This is all the more important in applications requiring high accuracy and, more importantly, requires there to be an understanding of how temperature may affect calibration and performance of the photometric systems. [11].

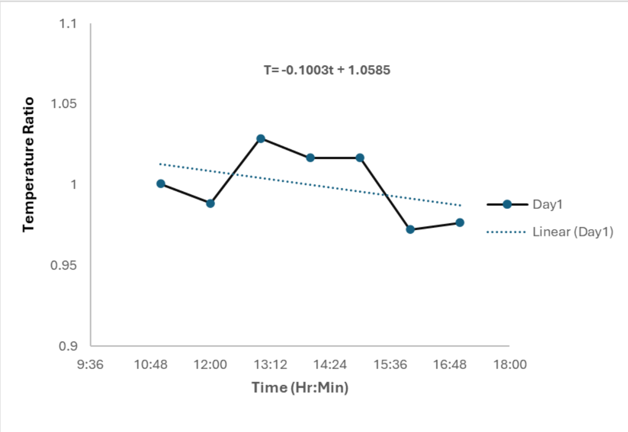


**Figure-8.** Illustrates the temperature fluctuations of the sphere photometer on the day one.

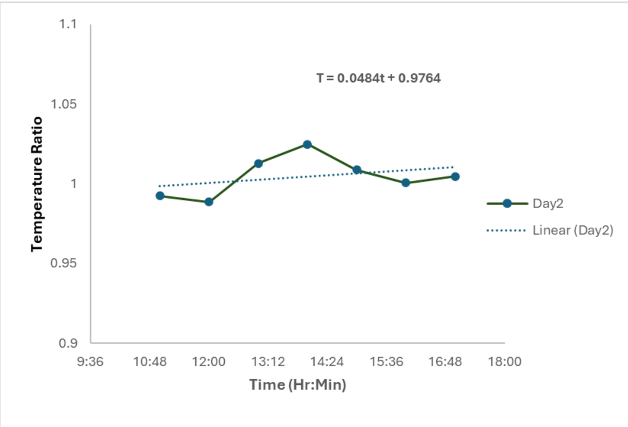


**Figure-9.** Illustrates the temperature fluctuations of the sphere photometer on the day two.

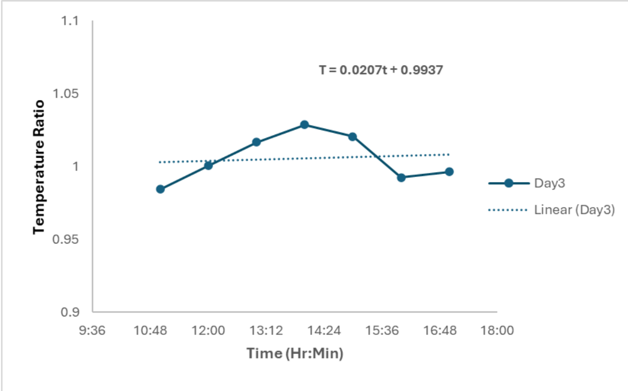


**Figure-10.** illustrates the temperature fluctuations of the sphere photometer on the day three.

These plots of Figures-8, 9, and 10 show the sphere photometer system temperature changes for the three days taken in the measurements. The data from the graphs above show the fluctuation of the temperature inside the sphere as time goes by; this is a very important cause of both the accuracy and stability of luminous flux measurements of the photometer. Figure-8 Temperature fluctuation on the first day: The above results indicate that the temperature fluctuation during the day reached 0.07 and therefore was not so stable. The problem could affect the whole performance because the variation in the temperature influences the sensitivity of the photometer and reduces its measurement repeatability. Figure 9 presents the results for the second day. The temperature variation for the day decreased slightly and remained within 0.05. A smaller fluctuation signifies that the temperature of the system's interior had started to settle, and the operating conditions were getting stabilized; therefore, the performance kept on improving. Figure-10 represents the temperature variation for the third day. The fluctuation further decreased, within 0.045, which means the system continued to stabilize. From the three days, the trend of the decrease in temperature variation tells that the system was reaching thermal equilibrium, which is very important to maintain the accuracy of the measurement. It was also observed that there was some temperature drift within each day. Further studies of these fluctuations showed that a linear trend in the temperature drift could be possible. This, in turn, allowed the research team to model, mathematically, the temperature variation of the sphere photometer as a simple linear drift, thus affording them a more accurate way of making corrections and adjustments in their sets of measurements. Indeed, the temperature variations for each of the three days, expressed by the following equations, could provide a mathematical framework that may be used for the purpose of predicting and making necessary compensations for drift in future measurements:

$$T = -0.1003t + 1.0585 \tag{4}$$

$$T = 0.0484t + 0.9764 \tag{5}$$

$$T = 0.0207t + 0.9937 \quad (6)$$

The Figures 8, 9 and 10 represent the temperature fluctuation in the sphere photometer system during the three days of measurement. Each of the equations in these three figures has two important variables - T and t. In this case, T describes the variation in temperature in the sphere photometer, while t is the time of calibration for the respective reading. These linear equations form the basis for understanding and accounting for the performance changes temperature causes in the sphere photometer. The slope of the equation gives an idea of how the temperature variation develops through time, while the intercept gives a reference to the initial temperature condition. These equations yield curves that are very useful in the fine-tuning of calibration procedures. With these equations, it would be rather easy to let the temperature drift over some time, start making some adjustments to the normal calibration calculations, and have the sphere photometer remain accurate in its results even at fluctuating temperatures. Refinement is necessary in such sensitive applications since any changes in temperature can determine the reliability of the data collected. By envelope curves of these temperature variation, detailed analysis would therefore permit better calibration practices, including real-time adjustments due to observed changes in temperature. The approach improves the accuracy in the sphere photometer system and ensures that the measurements obtained from this system are uncompromised by variability induced through changes in temperature.

## 4. UNCERTAINTY

It has to be the best way of assessing and stating measurement uncertainty flexibly, meaning applicable to all types of measurements and any input data. In such a method, the physical quantity representing uncertainty should be directly derived from its contributing components. The GUM insists that the measurement results should have been corrected for all significant systematic effects, and every reasonable effort should be made to identify and deal with such effects [12]. In establishing the Sphere Photometer Calibration Factor (SPCF), an all-encompassing method is applied that involves the incorporation and averaging of various measurement factors. These include: Repeatability of NIS Lamps: The SPCF takes the variability in lamp performance and ensures that the calibration is reproducible, with repeated measurements of Transfer Standard Lamps. Spatial Non-Uniformity of the Sphere: This accounts for the various light distributions across the integrating sphere. These particular spatial inhomogeneities can have effects on the accuracy of the measurement; therefore, these are included in the uncertainty budget. Lamp Output Distribution: Variations in the light output of various lamps are considered to provide a proper representation by the SPCF. Near-Field Absorption: Radiation absorption by lamp sockets and holders is accounted for. Since the same components are used throughout for all the lamps being compared, the variability in near-field absorption tends to remain constant and hence manifests itself in the uncertainty of the SPCF. Temperature Effects: Changes in temperature will, to a large extent, affect the coating reflectance of the sphere and the detector itself. A change in temperature can alter the reflective properties of the sphere coating and affect the response of the detector, thereby affecting the accuracy of measurement in its totality. The uncertainty in the SPCF value was obtained through a linear least-squares analysis and gives an estimate of 0.05% uncertainty in the SPCF. In the measurement of spectra, a spectroradiometer is used, for which the associated uncertainty as high as 4.7% is plausible. This gives, by comparison, a measure of the precision with the determination of the SPCF against other measurement devices.

**Table-2.** The uncertainty analysis of luminous flux measurements

| Uncertainty Budget | Relative standard uncertainty | Type of uncertainty |
|---|---|---|
| Standard lamp | 0.35 | B |
| Standard photometer | 0.25 | B |
| A drift of standard photometer | 4E-04 | B |
| Current measurements (Reference source) | 5E-02 | B |
| Current measurements (Test source) | 5E-02 | B |
| Photometer's nonlinearity | 1E-04 | B |
| The temperature of the IS | 0.045 | B |
| Repeatability of the measurements (Reference source) | 1E-02 | A |
| Repeatability of the measurements (Test source) | 3E-02 | A |
| Sphere photometer calibration factor (SPCF) | 0.05 | A |
| Expanded uncertainty (k=2) | 1.49 | |

## 5. CONCLUSIONS

The research presented has the calibration of the integrating sphere system applicable in measuring total luminous flux and assessing its uncertainty. It has been possible to determine very well the spectral responsivity of the sphere-photometer, which forms an essential variable for interpreting measurement results while estimating future uncertainties. In this way, it is ensured that the system of an integrating sphere will be correctly calibrated and able to perform a valid luminous flux measurement. A linear least-squares fit of the calibration factors with time, collected for each measurement day, was applied in order to get the final SPCF. The method gave a far more precise SPCF from the analysis of calibration data and fitted it to a linear model. The obtained SPCF is representative of the accuracy in the system calibration and is estimated to be within an uncertainty limit of about 0.03 to 0.05% over the period of measurement. A low level of uncertainty indicates the high degree of precision in the calibration process. Determination of SPCF included incorporation and averaging of many different measurement factors. It included repeatability assessment of NIS Incandescent standard lamps that were measured many times to ensure identical measurement results were obtained. The sphere spatial non-uniformity and the effects of lamp output distribution were assessed as well. In integrating these, the SPCF calibration process makes the necessary allowances for potential variations in measuring such that the possibilities of errors were avoided. The SPCF uncertainty also reflects the differences in the near-field absorption by lamp sockets and holders that can affect the measurements. These variations are included in the overall uncertainty assessment to provide a more realistic presentation of the reliability of the calibration factor. Other important findings of the study were the SPCF measurements that drifted in time due to the lack of temperature control both in the photometer and lamp during burning. This drift demonstrates how temperature management is one of the critical factors in SPCF calibration accuracy. During the measurement, the fluctuations in the temperature were measured within the measurement period and ranged from 0.045% to 0.07%. The variation cited above is an indication that the temperature needs control in order to limit its effects on the uncertainty of measurement.

## REFERENCES

[1] M. A. Haridy and A. Aslam. 2018. Optical Radiation Metrology and Uncertainty. In Metrology, InTech. 75205, pp. 75-92.

[2] CIE 127-2007, Measurement of LEDs, $2^{nd}$ ed. _Commission Internationale de l’Eclairage, Vienna, Austria, 2007.

[3] C. C. Miller and Y. Ohno. 2001. Proceedings of the Second CIE Expert Symposium on LED Measurement, Gaithersburg, MD. p. 45.

[4] K. Godo, T. Saito, H. Shitomi, T. Zama, and I. Saito. 2005. Proceedings of the NEWRAD2005. p. 199.

[5] Ohno Y. 1996. Photometry Calibration. NIST Special Publication 250-37.

[6] 1987. CIE Publication No. 84, Measurements of Luminous Flux.

[7] T. Poikonen, P. Manninen, P. Kärhä and E. Ikonen. 2010. Multifunctional Integrating Sphere Setup for Luminous Flux Measurements of Light Emitting Diodes. Rev. Sci. Instrum. 81, 023102.

[8] A. Alkermelawi, A. Alkamel, Manal A. Haridy. 2023. Development, and Uncertainty Evaluation of Luminous Flux Integrating Sphere Photometer System at NIS-Egypt. AIP Conf. Proc. 2620, 050001, MARCH 24.

[9] Manal A. Haridy. 2015. Improvement of the uncertainty of total luminous flux measurements by determining some correction factors. Int. J. Curr. Res. Aca. Rev. 3(6): 264-274.

[10] Manal. A. Haridy. 2008. The Realization of Luminous Flux Scale and Its Application in Preparing Calibrated and Tested Lamps. Doctoral thesis, college of Women, Ein Shams University, Egypt, and NRC Canada.

[11] Yoshi Ohno. 1997. Handbook of Applied Photometry. Measurement Procedures. American Institute of Physics, Woodbury, New York.

[12] Guide to the Expression of Uncertainty in Measurement, First Edition, International Organization for Standardization (ISO). 1995.